Title: Oxygen concentration modulates colibactin production

Authors : Nadège Bossuet $* [1], Cécile Guyonnet* [1], Camille V Chagneau [1,2], Min Tang-Fichaux [1], Marie Penary [1], Dorian Loubet [1], Priscilla Branchu [1], Eric Oswald [1,2], Jean-Philippe Nougayrede [1#]

** equal contribution*

1 IRSD, Université de Toulouse, INSERM, INRAE, ENVT, Univ Toulouse III Paul Sabatier (UPS), Toulouse, France

2 CHU Toulouse, Hôpital Purpan, Service de Bactériologie-Hygiène, Toulouse, France.

$ Orcid: 0000-0002-8215-1464

Orcid: 0000-0002-6802-1890. Correspondence: jean-philippe.nougayrede@inrae.fr

Abstract :

Up to 25% of the *E. coli* strains isolated from the feces of healthy humans harbor the *pks* genomic island encoding the synthesis of colibactin, a genotoxic metabolite. Evidence is accumulating for an etiologic role of colibactin in colorectal cancer. Little is known about the conditions of expression of colibactin in the gut. The intestine is characterized by a unique oxygenation profile, with a steep gradient between the physiological hypoxic epithelial surface and the anaerobic lumen, which favors the dominance of obligate anaerobes. Here, we report that colibactin production is maximal under anoxic conditions and decreases with increased oxygen concentration. We show that the aerobic respiration control (ArcA) positively regulates colibactin production and genotoxicity of *pks*+ *E. coli* in response to oxygen availability. Thus, colibactin synthesis is inhibited by oxygen, indicating that the *pks* biosynthetic pathway is adapted to the anoxic intestinal lumen and to the hypoxic infected or tumor tissue.

Keywords

Escherichia coli, colibactin, DNA damage, oxygen, hypoxia

Introduction

E. coli strains isolated from the feces of healthy subjects or from extra-intestinal infections, frequently harbor the *pks* genomic island that allow synthesis of a genotoxin called colibactin (1). This 54 kb *pks* island encodes a complex biosynthesis pathway, with polyketide synthases (PKS) and nonribosomal peptide synthetases (NRPS) as well as maturation enzymes, which cooperatively synthesize colibactin (2). Colibactin is an unstable peptide-polyketide metabolite, sensitive to aerobic oxidation and subsequent inactivation (3). Although colibactin is not directly purifiable, its bioactivity has been demonstrated in infected epithelial cells or on DNA exposed to *pks*+ bacteria: colibactin binds covalently to both strands of the DNA helix, resulting in interstrand crosslinks (4–6). Because these DNA lesions are highly toxic, the *pks* island also encodes self-protection systems (such as the ClbS protein) to protect the producing bacterium from the toxin (7–9). Colibactin is also toxic to the bacteria in the microbial community (10, 11) and to host mammalian cells. Epithelial cells exhibit DNA damage, cell cycle arrest, senescence and death upon exposure to *pks*+ bacteria (12, 13). Colibactin induces apoptotic cell death in lymphocytes and promotes virulence of *pks*+ *E. coli* during sepsis and meningitis (14–16). Colibactin is also produced in the gut by *pks*+ *E. coli* and inflicts DNA damage in intestinal epithelial cells (17–19). This DNA damage can ultimately lead to gene mutagenesis, and colibactin is suspected of promoting colon cancer (2, 17, 18). In mouse models that recapitulate intestinal tumorigenesis, inflammation is essential for cancer promotion by *pks*+ *E. coli*, and inflammation increases the transcription of *pks*-encoded genes (18, 20, 21). Thus, these bacteria appear to promote cancer under specific environmental conditions that favor expression of colibactin.

Recent studies have highlighted how environmental conditions regulate colibactin expression in *pks*+ *E. coli*. Indeed, it has been shown that colibactin production is regulated by iron availability (22). Factors originating from the producing bacterium or the host diet also modulate genotoxin production. The polyamine spermidine from bacterial metabolism or the environment is required for colibactin production (23). Similarly, carbon source impacts *pks* gene expression through regulation of central carbon metabolism (24). Oligosaccharides known to regulate bacterial metabolism increase colibactin expression, but this effect is abrogated by ferrous sulfate supplementation (25). Together, these studies suggest that colibactin production is constrained by the conditions in the bacterial microniche in the intestinal lumen.

The concentration of molecular oxygen (O_2, hereafter referred to as oxygen) is a key environmental factor in the gut, playing a central role in metabolic processes of both the host

62 and intestinal bacteria. The intestinal niche exhibits low oxygen tension, with a steep gradient
63 from anoxia in the lumen to physiological hypoxia at the epithelial surface (26). Oxygen serves
64 as an environmental cue for *E. coli*, with the Anoxic Redox Control (or Aerobic Respiration
65 Control; Arc) system detecting oxygen deprivation to regulate the expression of anaerobic
66 adaptation genes (27). The physiological hypoxia in the gut can be disrupted during disease,
67 such as at sites of mucosal inflammatory lesions, or in tumors, which can be deeply hypoxic
68 (28, 29) . On the other hand, chronic inflammation results in increased epithelial oxygenation
69 favoring aerobic proliferation of *E. coli* (30, 31). This has led to the hypothesis that oxygenation
70 of the intestinal niche is an important factor in the carcinogenic activity of *pks*+ *E. coli* (31).
71 The possibility that oxygen may directly modulate colibactin production by *pks*+ *E. coli* has
72 not yet been studied. In this paper, we report the serendipitous observation that oxygenation of
73 the bacterial culture has a marked impact on the toxicity of the genotoxin on the producing
74 bacterium. We further demonstrate that oxygen inhibits colibactin production and genotoxicity
75 in infected epithelial cells, and that the Arc system is a positive regulator of colibactin
76 production.

77

78

79 **Results**

80

81 **Oxygen inhibits colibactin autotoxicity in a colibactin-producing *E. coli clbS* mutant**

82

83 The colibactin biosynthetic pathway encodes self-protective systems, including the ClbS
84 protein that hydrolyzes colibactin and protects the *E. coli* genome DNA from colibactin toxicity
85 (7, 8). We previously observed that a laboratory K12 strain of *E. coli* transformed with a BAC
86 harboring the *pks* island with a deleted *clbS* gene exhibits an autotoxicity phenotype, with
87 impaired growth compared to the control strain harboring the intact *pks* island (8). While
88 studying this *clbS* mutant, we fortuitously observed that its autotoxicity phenotype was sensitive
89 to specific culture conditions. In particular, we noticed that the use of culture tubes with tightly
90 or loosely closed caps resulted in autotoxicity or normal growth, respectively. Based on this
91 observation, we found that the *clbS* mutant showed a significant ~10-fold decrease in CFU
92 count compared with wild-type or complemented mutant strains when grown in small closed
93 tubes, but not in large open tubes (Figure 1A). We thought that differences in culture
94 oxygenation were a likely explanation for this observation. To confirm a role of oxygen in the

95 expression of the *clbS* mutant autotoxicity phenotype, we tested cultures under atmospheric or
96 hypoxic conditions. Culture tubes with vented caps were incubated with agitation in a standard
97 atmosphere incubator (21% O_2) or in a dedicated hypoxic chamber with a 0.1% O_2 atmosphere.
98 In the hypoxic chamber, the *clbS* mutant showed a marked decrease of approximately 100-fold
99 in CFU numbers compared with the wild type or the complemented mutant (Figure 1B). In
100 contrast, the *clbS* culture in the 21% O_2 incubator did not show such a decrease in growth.
101
102 **Oxygen inhibits DNA-crosslinking by *pks+ E. coli***
103 The reduced autotoxicity phenotype in the *clbS* mutant exposed to high oxygen concentration
104 suggested that colibactin production, and/or its genotoxic activity, was inhibited. We therefore
105 examined the effect of various oxygen concentrations on colibactin production and activity.
106 Mature colibactin cannot be purified, but its genotoxicity can be detected by its DNA cross-
107 linking activity on exogenous DNA exposed to *pks+ E. coli* bacteria (4). We used the human
108 clinical *pks+ E. coli* strain SP15, which has been previously shown to produce colibactin in the
109 mouse intestinal lumen (17, 31) and to alter the gut microbiota through the production of
110 colibactin (32). DNA cross-linking activity of *E. coli* strain SP15 on linear DNA was tested at
111 different oxygen concentrations (0-21%). DNA cross-linking by colibactin was readily detected
112 at low (<1%) oxygen concentrations but decreased markedly at higher (4 and 13%)
113 concentrations, becoming undetectable at 21% O_2 (Figure 2AB). The growth of *E. coli* strain
114 SP15 was similar regardless of oxygen concentration (Figure 2C), indicating that the
115 modulation of its cross-linking activity was not explained by the number of bacteria. Thus,
116 oxygen inhibits the activity and/or production of colibactin.
117
118 **Oxygen inhibits the expression and production of colibactin by *pks+ E. coli***
119 To examine whether oxygen modulates colibactin production, we quantified the metabolite N-
120 myristoyl-D-AsnOH (C14-Asn), a stable byproduct released during the final step of colibactin
121 synthesis (9). *E. coli* strain SP15 was grown as before with different oxygen concentrations,
122 lipids were extracted from the culture supernatants and analyzed by quantitative
123 chromatography coupled to mass spectrometry. C14-Asn production by SP15 was highest at
124 low oxygen concentrations (<1% O_2) and decreased at higher concentrations, with only
125 background levels at 13 and 21% O_2 (Figure 3). Thus, the synthesis of colibactin was the highest
126 at low oxygen concentration but diminished with increasing oxygen concentration.
127 To confirm that oxygen inhibits colibactin synthesis, we measured the activity of the
128 promoter of *clbB*, which encodes one of the key NRPS-PKSs in the synthesis pathway (33). *E.*

129 *coli* strain SP15 harboring a luciferase reporter system under the control of either a known
130 constitutive promoter or the *clbB* promoter was grown with different oxygen concentrations,
131 and then luminescence was quantified (Figure 4). The constitutive promoter showed no
132 significant change in activity at all oxygen concentrations, whereas the *clbB* promoter showed
133 its highest activity in anoxic cultures, and decreasing activity with increasing oxygen
134 concentration (Figure 4). This result is consistent with a recent report of increased transcription
135 of a *clbB-lacZ* reporter under oxygen-limited conditions (10). To confirm this finding, we
136 measured by quantitative PCR the expression of the *clbB* gene and that of a control reference
137 gene. We found that *clbB* mRNA expression was highest in anoxic cultures and decreased with
138 increasing oxygen concentration (Figure 5). Together with the observation that DNA cross-
139 linking activity and colibactin autotoxicity are inhibited by oxygen, these results demonstrated
140 that oxygen constrains colibactin production.
141
142 **ArcA is required for full DNA-crosslinking by *E. coli* producing colibactin**
143 We next sought to investigate the mechanism by which oxygen regulates colibactin production.
144 The ArcAB two component system, composed of the ArcB sensor and the response regulator
145 ArcA, is well known to sense microaerobic and anaerobic conditions (27). To test for a role in
146 colibactin production, we constructed a SP15 strain mutated for *arcA* and assessed its DNA
147 cross-linking activity at a low (0.1%) oxygen concentration (Figure 6). The DNA cross-linking
148 activity of the *arcA* mutant was significantly reduced compared to the wild-type strain, and was
149 restored in the mutant hosting a plasmid-encoded *arcA* gene (Figure 6A and B). The growth of
150 *E. coli* wild-type strain SP15, *arcA* mutant and complemented mutant strain was similar (Figure
151 6C), indicating that the altered cross-linking activity of the *arcA* mutant was not due to a growth
152 defect and reduced bacterial numbers.
153
154 **ArcA positively regulates the expression of *clbB***
155 The *arcA* mutant exhibited a significantly reduced *clbB* promoter activity compared to the wild-
156 type strain (Figure 7A). In contrast, a *clbP* mutant defective in colibactin production (34)
157 showed wild-type levels of promoter activity, indicating that colibactin production does not
158 indirectly regulate *clbB* promoter activity. The activity of the *clbB* promoter was significantly
159 reduced in a *clbP arcA* double mutant, as in the single *arcA* mutant (Figure 7A). However,
160 neither the mutation of *arcA* and/or *clbP*, nor the oxygen concentration altered the activity of a
161 constitutive control or *clbS* promoter (supplementary figure 1), indicating that ArcA
162 specifically affects ClbB expression. We confirmed by Q-PCR that *clbB* mRNA expression was

163 significantly reduced in the *arcA* mutant or the *clbP arcA* double mutant (Figure 7B). These
164 results suggest that ArcA positively regulates the *clbB* gene under low oxygen conditions.
165 To determine whether this regulation is direct or indirect, we searched for ArcA-binding sites
166 within the *clbB* promoter region. Using the *in silico* PRODORIC virtual footprint tool (35), a
167 putative ArcA binding site was located at position -39 (TGTTAAATAA, score 0.99) upstream
168 of the ClbB open reading frame. We next performed an electrophoretic mobility shift assay
169 (EMSA) using a DNA fragment containing the *clbB* promoter region and purified ArcA protein,
170 which was phosphorylated or not. ArcA is converted to its active form by phosphorylation by
171 ArcB to allow binding to the promoter region of target genes (27). Phosphorylated ArcA
172 induced a dose-dependent band shift of the *clbB* DNA probe (Figure 8). In contrast, non-
173 phosphorylated ArcA induced a much smaller band shift, in agreement with similar
174 observations at other ArcA-regulated promoters (36). A similar small non-specific band shift
175 was observed with a DNA fragment amplified from the coding region of *cysG* as a negative
176 control, while the promoter region of *mdh* which is a known ArcA-binding locus (37), showed
177 a strong band-shift similar to that of the *clbB* probe when bound to phosphorylated ArcA
178 (Figure 8). Taken together, these results indicate that ArcA regulates the production of
179 colibactin in a positive and direct manner.
180
181
182 **Oxygen and *arcA* mutation inhibit the genotoxicity of *pks*+ *E. coli* infecting epithelial cells**
183 To confirm that oxygen inhibits colibactin production, we examined the genotoxicity of the *E.*
184 *coli* strain SP15 in epithelial cells grown in a standard atmosphere (21% O_2) or in "physioxic"
185 conditions (4% O_2) (38). Human epithelial HeLa cells were infected 4 hours with the bacteria,
186 at 21% or 4% O_2, then DNA damage was visualized 4 hours later by immunofluorescence
187 staining of histone H2AX S139-phosphorylation (γH2AX) (1) (Figure 9). Infection with SP15
188 at 21% oxygen inflicted detectable, low-level DNA damage, while infection at 4% oxygen
189 induced markedly higher DNA damage (Figure 9AB). HeLa cells treated with genotoxic
190 cisplatin under 21% or 4% oxygen conditions had similar γH2AX levels, indicating that a
191 modulation of the DNA damage response by oxygen cannot account for the increased
192 genotoxicity of SP15 at 4% oxygen (Supplementary figure 2). We also assessed the
193 genotoxicity of the *arcA* mutant in physioxic conditions. The mutant induced significantly
194 reduced DNA damage, while the complemented mutant had its genotoxicity restored (Figure

195 9AB). In contrast, the *clbP* mutant and *clbP arcA* double mutant were both non-genotoxic, with
196 cells exposed to these mutants showing baseline levels of γH2AX (Figure 9AB).
197 To strengthen these results, the genotoxicity of the wild-type and mutant strains was tested on
198 non-transformed rat intestinal epithelial cells (IEC-6) at 21 or 4% O_2. The results were similar
199 to those in HeLa cells, with an increase in the genotoxicity of *E. coli* SP15 at 4% compared to
200 21% O_2, which was reduced in the *arcA* mutant, and abolished in the *clbP* and *clbP arcA*
201 mutants (supplementary figure 3). We also examined the cytotoxicity of *pks+ E. coli* in HeLa
202 and IEC-6 cells at 21 or 4% O_2. Indeed, the cellular response to DNA damage induced by
203 colibactin leads to proliferation arrest, cell death and senescence, resulting in reduced cell
204 numbers and the formation of giant cells (megalocytosis) (13). In both cell lines, this
205 cytotoxicity phenotype induced by the wild-type and mutant strains followed that of the
206 genotoxicity observed with the same strains; the cytotoxicity of the wild-type SP15 was greater
207 in physioxia, and markedly reduced in the *arcA* mutant, whereas it was restored in the
208 complemented *arcA* mutant, but completely abolished in the *clbP* mutant or the *clbP arcA*
209 double mutant (Supplementary figure 4).

210 Overall, our data show that oxygen concentration modulates colibactin production and
211 genotoxic activity of *pks+ E. coli* on epithelial cells via an *arcA*-dependent mechanism.

212

213 **Discussion**

214

215 We show that oxygen reduces the production and genotoxicity of colibactin, and that the Arc
216 system which sense oxygen availability positively regulates colibactin production. This
217 regulation of colibactin production is consistent with the observation that fitness and virulence
218 systems of enterobacteria are usually regulated by oxygen (27). Indeed, commensal as well as
219 pathogenic enterobacteria encounter oxygen levels that are generally hypoxic, with steep
220 gradients and dynamic oxygenation cycles. Natural oxygenation conditions are in sharp contrast
221 to the constant, high oxygen concentration used in standard "normoxic" (21% O_2) *in vitro*
222 experiments. In contrast, the intestine exhibit longitudinal and cross-sectional gradients of
223 oxygen concentration, decreasing from the small to the large intestine, and increasing from the
224 anoxic (<0.1% O_2) lumen to the oxygenated (~1% O_2) epithelium surface (39). Intestinal
225 oxygenation further fluctuates between rest and ingestion of nutrients, when absorptive
226 hyperemia occurs. Besides the intestinal niche, in the host epithelial tissues and fluids (such as

227 urine), pathogenic enterobacteria encounter "physioxic" oxygen levels (2% to 9%, averaging
228 ~4%) (38, 40). Pathogenic enterobacteria such as *Shigella*, enterotoxigenic *E. coli*, avian and
229 uropathogenic *E. coli* tightly regulate the expression of their virulence factors in relation to
230 oxygen concentration (41–44). For *pks*+ *E. coli*, the regulation of colibactin production by
231 oxygen via the Arc system could be viewed as a selected advantage in relation with the
232 regulation of virulence and fitness within the host. Indeed, the metabolic cost of synthesizing a
233 complex compound such as colibactin using eight huge NRPS and PKS enzymes is very high,
234 implying that the selective pressure for their expression and maintenance must be strong (45).
235 As colibactin is susceptible to aerobic oxidation (3), an energy saving strategy that inhibits its
236 synthesis under environmental oxygen conditions leading to its inactivation may have been
237 selected. Alternatively, the adaptation of colibactin bioactivity and production to a low-oxygen
238 environment could be associated to the role of colibactin in the competition with the
239 polymicrobial community in the anoxic intestinal lumen. Indeed, recent findings highlighted a
240 direct role for colibactin in killing or inhibiting enteric bacteria (such as the anaerobe
241 *Bacteroides fragilis*), in the induction of prophages in polymicrobial enteric anerobic cultures,
242 and ultimately in shaping the gut microbiota (10, 11, 32). Our finding that an anoxic
243 environment is most favorable for colibactin production is thus consistent with the recently
244 proposed role of colibactin in interbacterial competition in gut lumen.

245 The notion that oxygen regulates colibactin production is also relevant to the question
246 of whether, where and when colibactin inflicts DNA damage in the gut. It has been repeatedly
247 reported that DNA damage was inflicted in enterocytes of rats and mice colonized or force-fed
248 with different strains of *E. coli pks*+ (NC101, 192PP, M1/5, SP15, 11G5, the probiotic strain
249 Nissle 1917) (15, 17, 19, 20, 46, 47). Keeping in mind that colibactin production is also
250 regulated by a variety of environmental cues such as iron, polyamines, and carbon sources (22–
251 24), the physiological hypoxia at the surface of the epithelium could constitute a favorable
252 environment for colibactin production and activity. Consistent with this hypothesis, we
253 observed in this work that *E. coli* SP15 induced marked DNA damage under physioxic
254 conditions in two epithelial cell lines. Other low oxygen intestinal compartments could favor
255 even more colibactin production, such as the stem cells that reside in a hypoxic niche (as low
256 as 1% O_2) at the bottom of the crypt (48). Signs of long-term persistent chromosomal instability
257 have been reported in animals colonized with *pks*+ *E. coli* (46) and the mutational signature of
258 colibactin has been found in intestinal crypts in healthy human subjects (49), suggesting that
259 *pks*+ *E. coli* could leave their genotoxic imprint in stem cells. As far as is described in the
260 literature, *E. coli pks*+ have not yet been observed in the gut stem niche, but were shown to

261 form biofilms together with the anaerobe *B. fragilis* on the colonic epithelium of colorectal
262 cancer patients (50). It is well known that tumor tissue is hypoxic compared to healthy tissue
263 (29), and thus could present another favorable environment for colibactin production. It is also
264 interesting to note that inflammation appears to be a key factor in promoting colorectal
265 tumorigenesis by *E. coli pks*+ in mouse models (18, 20). Severe inflammation can lead to local
266 oxygen depletion, resulting from tissue necrosis and neutrophil respiratory burst (28). Such
267 hypoxic areas can also be generated during infectious processes, when the host responds by
268 coagulation to prevent bacterial dissemination, thus generating a rapid drop in local oxygen
269 tension (51). Hypoxia at the level of the inflamed and infected tissues could therefore present
270 environments favorable for colibactin production. Further study of the localization of *pks*+
271 bacteria in relation to host cell DNA damage and tissue inflammation will be necessary to better
272 understand the impact of colibactin on infection and cancer.
273 In conclusion, we provide evidence that oxygen decreases colibactin synthesis by *E. coli*
274 via an *arcA*-dependent regulatory mechanism, raising the hypothesis that colibactin production
275 and genotoxic activity are adapted to the bacterial warfare in the anoxic gut and also to hypoxic
276 infected, inflamed and tumor tissues.
277
278
279
280 **Materials and Methods**
281
282 **Bacterial strains, mutants, plasmids and primers**
283 The bacterial strains, plasmids and primers used in this study are listed in Table 1. Mutagenesis
284 of *arcA* gene was performed by using the lambda red mutagenesis method, and confirmed by
285 PCR, with the primers listed in Table 1. The mutant was trans-complemented with the pGEN-
286 arcA plasmid. The plasmid pMT20 was constructed by PCR amplification of the 740 bp DNA
287 sequence upstream of the *clbS* gene from the SP15 genome, and cloned into the reporter plasmid
288 pCM17 encoding the *luxCDABE* operon. The resulting plasmid was verified by sequencing.

Strains, plasmids, primers	**Genotype, use, sequence**	**Reference**
Strains		

E. coli DH10B pBACpks	DH10B strain carrying the *pks*-island on a pBeloBAC11 vector		(1)
DH10B pBACpks *clbS*	*clbS::FRT* mutant		(8)
E. coli SP15	Clinical *E. coli* O18:K1 *pks*+ strain, isolated from the spinal fluid of a neonate with meningitis		(17)
E. coli SP15 *arcA*	*arcA::kan* mutant		This study
E. coli SP15 *clbP*	*clbP::FRT* mutant		(52)
E. coli SP15 *clbP arcA*	*arcA::kan clbP::FRT* double mutant		This study
Plasmids			
pClbS	Plasmid pASK75 carrying *clbS*		(8)
pCM17	Plasmid containing the *luxCDABE* operon driven by a constitutive promoter		(53)
pMT3	pCM17-derived plasmid containing the *luxCDABE* operon driven by the *clbB* promoter region		(33)
pMT20	pCM17-derived plasmid containing the *luxCDABE* operon driven by the *clbS* promoter region		This study
pGEN-arcA	Plasmid pGEN-MCS carrying *arcA*		(44)
pET28a-arcA6His	Plasmid for the expression and purification of 6His-tagged ArcA protein		(44)
Primers			
NG49	Standard range *clbB*	5'-AAACAACAAGGGGCTGACAC-3'	This study
NG50	Standard range *clbB*	5'-CAGTCAGCGCCACATGTAAG-3'	This study
NG61	Q-PCR *clbB*	5'-ACCGAATCAGTATGAAAACCAG-3'	This study

NG62	Q-PCR *clbB*	5'-GCACACTATCACTCCTCCAAC-3'	This study
NG53	Standard range *cysG*	5'-CGCCAGCTTTATTATGCCGT-3'	This study
NG54bis	Standard range *cysG,* EMSA negative control	5'-GTAGACCACCACATCTGCCT-3'	This study
NG55bis	Q-PCR *cysG*, EMSA negative control	5'-TGGGCCAGGTAGCGAA-3'	This study
NG56	Q-PCR *cysG*	5'-GGACCTGCACCAACCA-3'	This study
NG100	*clbB* promoter region EMSA	5'-TGGCAGTATTTAAGAGGAATTTACG-3'	This study
NG101	*clbB* promoter region EMSA	5'-TATCCATAACCATCACCTTATTATCG-3'	This study
NG104	*mdh* promoter EMSA positive control	5'- TGCGACTTTCATCCTAAACT-3'	This study
NG105	*mdh* promoter EMSA	5'- GGGTATATTGTCACCACCTG-3'	This study

	positive control		
PB60	Lambda red mutagenesis of *arcA*	5'-GGGACTTTTGTACTTCCTGTTTC GATTTAGTTGGCAATTTAGGTAGCAA ACGTGTAGGCTGGAGCTGCTTCG-3'	This study
PB61	Lambda red mutagenesis of *arcA*	5'-GAAAAATAAAAACGGCGCTAAAA AGCGCCGTTTTTATTGACGGTGGTAAA GCCGACATATGAATATCCTCCTTAGT -3'	This study
PB62	Verification of *arcA* mutant	5'-GCATCAGGCAGGTCAGGGAC-3'	This study
PB63	Verification of *arcA* mutant	5'-CCAGTAAAGAAGTTACCATGG-3'	This study
MT28_clbS-prom2F	Cloning of *clbS* promoter region	5'-CCGGAATTCCATATTCAGGTGGTTCTGC-3'	This study
MT10_clbS-prom1R	Cloning of *clbS* promoter region	5-CGCGGATCCGAACAGCCATATCTATTGCTCCTTG-3'	This study

289

290 **Bacterial culture conditions**

291 The day before the experiments, the *E. coli* strains were grown overnight in a standard incubator
292 at 37°C with 240 RPM shaking in Lennox L broth (LB, Invitrogen) supplemented when
293 required with appropriate antibiotics (Kanamycin 50 µg/ml, streptomycin 50 µg/ml,
294 chloramphenicol 25 µg/ml or carbenicillin 50 µg/ml). Then, the bacteria were pre-cultured in
295 LB or in Dulbecco's modified Eagle's medium (DMEM) with 25 mM HEPES (Invitrogen) to
296 reach the exponential phase (OD600 ~ 0.4). Cultures at various oxygen concentrations were
297 performed in a hypoxic workstation (Whitley H35) regulated at 0.1% to 13% O_2, 5% CO_2, 37°C
298 and 70-90% humidity. To achieve a 0% O_2 anoxic atmosphere, we used a jar with anaerobic

299 atmosphere generation bags (Sigma) manipulated within the hypoxic workstation set at 0.1%
300 oxygen. Standard microbiological and cell culture incubators were used for the 21% O_2
301 (atmospheric) condition. Culture media were equilibrated for 16-24 h at the required oxygen
302 concentration before use. For DH10B strains (Figure 1), LB cultures were inoculated with
303 $2x10^6$ bacteria/ml in 5 ml and grown overnight (17 h) in fully closed 10 ml tubes (Kima), or in
304 opened 50 ml tubes (Falcon), or in 14 ml 17x100 mm tubes with the cap in vented position
305 (Falcon 352059). The *E. coli* strain SP15 was inoculated ($1.5x10^7$ bacteria) in 1 ml DMEM
306 Hepes in Falcon 352059 tubes with the cap in vented position and cultivated 3.5 h with 240
307 RPM agitation at 37°C within the hypoxystation set at the oxygen concentration required. For
308 CFU enumeration, the cultures were serial-diluted in PBS, plated on LB agar plates and
309 incubated overnight at 37°C in a standard incubator.
310
311 **Exogenous DNA cross-linking by colibactin-producing *E. coli***
312 The assay was performed as described before (4). Briefly, 100µl of bacterial culture were added
313 with 500 ng DNA (pUC19 linearized by BamHI digestion) and 1mM EDTA, then incubated 40
314 min at the indicated oxygen concentration. The DNA was recovered using a Qiagen PCR
315 purification kit, analyzed by denaturing gel electrophoresis, stained with GelRed (Biotium) and
316 visualized with a Bio-Rad Chemidoc XRS system. DNA bands were quantified from
317 unsaturated flat-fielded images using ImageJ.
318
319 **Quantification of N-myristoyl-D-AsnOH (C14-Asn)**
320 Bacterial supernatants (1.5 ml) were prepared by centrifugation at 5000 g, filtration through
321 0.22 µm PVDF filters (Millipore) and stored at -80°C. Lipids were extracted and analyzed as
322 before (54): briefly, 1 ml of sample was extracted on solid phase 96 wells plates (OASIS HLB,
323 Waters), eluted with methanol, evaporated twice under N_2 then suspended in 10 µl methanol.
324 The quantification of C14-Asn was performed by the MetaToul Lipidomics facility (Inserm
325 UMR1048, Toulouse, France), using an in-house quantification assay by high-performance
326 liquid chromatography/tandem mass spectrometry analysis.
327
328 **Bioluminescence monitoring of *clbB* and *clbS* promoter activity**
329 The *E. coli* strain SP15 hosting pMT3, pMT20 or pCM17 (containing the *Photorhabdus*
330 *luminescens luxCDABE* operon driven by the *clbB* or *clbS* promoter region (33) or a constitutive
331 promoter (53) respectively) was cultivated at the required concentration of oxygen, then 100µl
332 were transferred on 96 wells black plates (Greiner), the plate was shaken vigorously 5 sec to

333 provide oxygen to the luciferase and the bioluminescence was measured with a Tecan Spark
334 plate reader or a Perkin Elmer EnSight multimode plate reader, or photographed with a Bio-
335 Rad Chemidoc XRS system.
336

337 ***clbB* mRNA quantification**

338 10^9 bacteria were collected by centrifugation and stored at -80°C. RNA was purified using the
339 RNA Easy plus mini kit (Qiagen), then 2 µg were used to synthesize cDNA with the i-script kit
340 (Bio-Rad). For standard range of *clbB* and *cysG* housekeeping gene (55), PCRs were performed
341 using *E. coli* SP15 genome as a template and the primer pairs NG49/NG50 and NG53/NG54
342 respectively. Standards were purified and serial diluted from 5.10^9 to 5.10^1 copy/µl. Real time
343 PCR were performed with the iQ SYBR Green supermix (Bio-Rad), with 2 µl of cDNA or
344 standard dilutions, and 187.5 nM of primer pairs NG61/NG62 (*clbB*) or NG55/NG56 (*cysG*).
345 The copy numbers of *clbB* and *cysG* were calculated from the Ct obtained using the standard
346 curves. The expression of *clbB* gene at different oxygen concentration was calculated by the
347 ratio *clbB* / *cysG* copy numbers and normalized at 100% by the mean at 0.1% oxygen.

348

349 **Epithelial cells infection, quantification of DNA-damage and megalocytosis assay**

350 The DNA-damage and megalocytosis assays were performed as described before (4, 52) with
351 some modifications. HeLa and IEC-6 cells were cultivated in a standard atmospheric 37°C 5%
352 CO_2 incubator, in DMEM Glutamax (Invitrogen) supplemented with 10% fetal calf serum
353 (FCS), 50 µg/ml gentamicin and 1% non-essential amino acids (Invitrogen). IEC-6 cells were
354 supplemented with 0.1 U/mL of bovine insulin (Sigma-Aldrich). The cells were seeded in 8-
355 chambers slides or in 96-wells plates (Falcon) and grown 24 hours in the atmospheric 5% CO_2
356 incubator, or in the hypoxic workstation set at 4% O_2 5% CO_2. The cells were infected in
357 DMEM 25 mM HEPES at a multiplicity of 100 bacteria per cell and incubated 4 hours in the
358 hypoxic or standard incubator. As controls, the cells were left uninfected or were treated with
359 20 µM cisplatin (Sigma) to induce DNA-damage. The cells were then washed 3 times with
360 HBSS supplemented with 100 µg/ml gentamicin, incubated in complete cell culture medium
361 supplemented with 100 µg/ml gentamicin for 4 hours, in the same hypoxic or standard
362 incubator. The cells were finally washed in PBS and fixed 15 min in PBS 4% formaldehyde.
363 Following 5 min permeabilization in 0.2% Triton X-100, and blocking in MAXblock medium
364 (Active Motif), the cells were stained with antibodies against γH2AX (1:500, JBW301,

365 Millipore) followed with anti-mouse AlexaFluor 488 (1:1000, Invitrogen). The cells were
366 mounted in Fluoroshield w/DAPI medium (Sigma), and examined with a Zeiss 710 laser
367 scanning confocal microscope at 63X. The mean fluorescence intensities of γH2AX within the
368 nuclei were analyzed using a NIH ImageJ macro: the nuclei were identified in the DNA image
369 and the mean fluorescence intensity of γH2AX was measured in the masked green channel for
370 each nucleus. The megalocytosis phenotype induced by colibactin was examined as previously
371 described (52). Briefly, HeLa and IEC-6 cells in were infected as above in the standard
372 atmospheric or hypoxic (4% oxygen) incubator, then washed and incubated with gentamicin
373 for 48 h before staining with methylene blue. The cells were photographed using an Olympus
374 BX41 microscope equipped with a 10x objective and a Leica DCF300FX camera.

375

376 **Purification, phosphorylation of ArcA-6His protein and electrophoretic mobility shift**
377 **assay (EMSA)**

378 ArcA-6His purification and phosphorylation were performed as described previously, with
379 some modifications (44). Briefly, *E. coli* BL21 pET28a-arcA6His was grown overnight at 28°C
380 in 100 ml of LB with 0.1 mM IPTG. Bacteria were lysed in equilibration buffer (20 mM
381 NaH_2PO_4, 300 mM NaCl, 10 mM imidazole, pH 8) supplemented with lysozyme and anti-
382 protease cocktail (Roche), followed by sonication. The lysate was cleared by centrifugation
383 (10000 g, 30 min) and the supernatant was loaded 1 h on HisPur Ni-NTA superflow agarose
384 (Fisher). The agarose was washed with equilibration buffer and eluted with increasing
385 imidazole concentration (25, 50, 100 mM). The eluate was dialyzed in 20 mM Tris 50 mM
386 NaCl 40 mM EDTA 4 mM dithiothreitol [DTT] 10% glycerol pH 7.4 buffer 16 h at 4°C with
387 three buffer changes. Then the protein sample was concentrated using an Amicon Ultra
388 centrifugal tube (Merck) with a buffer change to phosphorylation buffer 2X (100 mM Tris pH
389 8, 1mM EDTA, 20 mM glycerol, 20 mM $MgCl_2$). The protein sample was stored at 4°C.
390 Phosphorylation of 20 µg ArcA-6His was performed with 100 mM lithium potassium acetyl
391 phosphate in 1X phosphorylation buffer. A non-phosphorylated protein control was prepared
392 by omitting the lithium reagent. After incubation for 60 min at 25°C the samples were used
393 immediately for DNA binding assay.

394 EMSA was performed as previously described (44). Briefly, DNA probes with the promoter
395 regions of *mdh* as positive control, an intragenic region of *cysG* as negative control, and the
396 promoter region of *clbB* were generated by PCR using primers listed in table 1. DNA probes

397 were gel-purified (Qiagen kit), then 50 ng of DNA was mixed with increasing amounts of
398 phosphorylated ArcA-His (0 to 600 ng) or non-phosphorylated protein (600 ng) in binding
399 buffer (100mM Tris pH7.4, 10 mM $MgCl_2$, 5% glycerol, 400 µg/mg BSA, 2 mM DTT, 100
400 mM KCl) for 30 min at 37°C. The reaction mixtures were then subjected to electrophoresis on
401 a 6% polyacrylamide Novex TBE gel (Thermo) in 0.5× TBE Novex running buffer, at 200 V
402 for 45 min. The gel was stained in 0.5× TBE containing 1× SYBR Gold nucleic acid stain (Life
403 Technologies) for 30 min, and then the image was recorded using a ChemiDoc (BioRad).

404

405 **Statistical analyses**

406 For quantifications, three or four independent experiments were performed for each oxygen
407 concentration tested. CFU counts were log-transformed. Statistical analyses were performed
408 with GraphPad Prism v9. P values were calculated using ANOVA followed by Tukey post-
409 tests, or with a t-test.

410

411

412 **Acknowledgement**

413 We thank Dr. Ganwu Li for the gift of the pGEN-arcA and pET28a-arcA plasmids, and Simon
414 Lachambre & Lhorane Lobjois for technical assistance at the Infinity Cell Imaging Facility,
415 Toulouse.

416

417 **Funding information**

418 This work was supported by the French Agence Nationale de la Recherche under grants ANR-
419 17-CE35-0010, ANR-18-CE14-0039, ANR-19-CE34-0014. The hypoxystation used in this
420 work was sponsored by a grant from INRAE (to JPN) and the European Regional Development
421 Fund (to Dr. Nathalie Vergnolle, IRSD). CG and DL received an inter-regional "research year"
422 scholarship (South-West France, pharmacy field).

423

424 **Disclosure statement**

425 The authors report there are no competing interests to declare.

426

427 **Data availability statement**

428 The authors confirm that the data supporting the findings of this study are available within the
429 article.

430

431 **References**

432 1. Nougayrède J-P, Homburg S, Taieb F, Boury M, Brzuszkiewicz E, Gottschalk G,
433 Buchrieser C, Hacker J, Dobrindt U, Oswald E. 2006. Escherichia coli induces DNA double-
434 strand breaks in eukaryotic cells. 5788. Science 313:848–51.

435 2. Chagneau CV, Payros D, Tang-Fichaux M, Auvray F, Nougayrède J-P, Oswald E.
436 2022. The pks island: a bacterial Swiss army knife? Colibactin: beyond DNA damage and
437 cancer. Trends Microbiol 30:1146–1159.

438 3. Wernke KM, Xue M, Tirla A, Kim CS, Crawford JM, Herzon SB. 2020. Structure and
439 bioactivity of colibactin. Bioorg Med Chem Lett 30:127280.

440 4. Bossuet-Greif N, Vignard J, Taieb F, Mirey G, Dubois D, Petit C, Oswald E,
441 Nougayrède J-P. 2018. The Colibactin Genotoxin Generates DNA Interstrand Cross-Links in
442 Infected Cells. 2. mBio 9:e02393-17.

443 5. Xue M, Kim CS, Healy AR, Wernke KM, Wang Z, Frischling MC, Shine EE, Wang
444 W, Herzon SB, Crawford JM. 2019. Structure elucidation of colibactin and its DNA cross-
445 links. Science 365.

446 6. Wilson MR, Jiang Y, Villalta PW, Stornetta A, Boudreau PD, Carrá A, Brennan CA,
447 Chun E, Ngo L, Samson LD, Engelward BP, Garrett WS, Balbo S, Balskus EP. 2019. The
448 human gut bacterial genotoxin colibactin alkylates DNA. Science 363.

449 7. Tripathi P, Shine EE, Healy AR, Kim CS, Herzon SB, Bruner SD, Crawford JM.
450 2017. ClbS Is a Cyclopropane Hydrolase That Confers Colibactin Resistance. 49. JOURNAL
451 OF THE AMERICAN CHEMICAL SOCIETY 139:17719–17722.

452 8. Bossuet-Greif N, Dubois D, Petit C, Tronnet S, Martin P, Bonnet R, Oswald E,
453 Nougayrède J-P. 2016. Escherichia coli ClbS is a colibactin resistance protein. 5. Mol
454 Microbiol 99:897–908.

455 9. Brotherton CA, Balskus EP. 2013. A prodrug resistance mechanism is involved in
456 colibactin biosynthesis and cytotoxicity. 9. J Am Chem Soc 135:3359–3362.

457 10. Chen J, Byun H, Liu R, Jung I-J, Pu Q, Zhu CY, Tanchoco E, Alavi S, Degnan PH,
458 Ma AT, Roggiani M, Beld J, Goulian M, Hsiao A, Zhu J. 2022. A commensal-encoded
459 genotoxin drives restriction of Vibrio cholerae colonization and host gut microbiome
460 remodeling. Proc Natl Acad Sci U S A 119:e2121180119.

461 11. Silpe JE, Wong JWH, Owen SV, Baym M, Balskus EP. 2022. The bacterial toxin
462 colibactin triggers prophage induction. Nature 603:315–320.

463 12. Faïs T, Delmas J, Barnich N, Bonnet R, Dalmasso G. 2018. Colibactin: More Than a
464 New Bacterial Toxin. Toxins (Basel) 10:E151.

465 13. Secher T, Samba-Louaka A, Oswald E, Nougayrède J-P. 2013. Escherichia coli
466 producing colibactin triggers premature and transmissible senescence in mammalian cells.
467 PLoS One 8:e77157.

468 14. Marcq I, Martin P, Payros D, Cuevas-Ramos G, Boury M, Watrin C, Nougayrède J-P,
469 Olier M, Oswald E. 2014. The genotoxin colibactin exacerbates lymphopenia and decreases
470 survival rate in mice infected with septicemic Escherichia coli. 2. J Infect Dis 210:285–294.

471 15. McCarthy AJ, Martin P, Cloup E, Stabler RA, Oswald E, Taylor PW. 2015. The
472 Genotoxin Colibactin Is a Determinant of Virulence in Escherichia coli K1 Experimental
473 Neonatal Systemic Infection. 9. Infect Immun 83:3704–3711.

474 16. Wang P, Zhang J, Chen Y, Zhong H, Wang H, Li J, Zhu G, Xia P, Cui L, Li J, Dong J,
475 Gao Q, Meng X. 2021. Colibactin in avian pathogenic Escherichia coli contributes to the
476 development of meningitis in a mouse model. Virulence 12:2382–2399.

477 17. Cuevas-Ramos G, Petit CR, Marcq I, Boury M, Oswald E, Nougayrède J-P. 2010.
478 Escherichia coli induces DNA damage in vivo and triggers genomic instability in mammalian
479 cells. 25. Proc Natl Acad Sci USA 107:11537–11542.

480 18. Dougherty MW, Jobin C. 2021. Shining a Light on Colibactin Biology. Toxins (Basel)
481 13:346.

482 19. Nougayrède J-P, Chagneau CV, Motta J-P, Bossuet-Greif N, Belloy M, Taieb F,
483 Gratadoux J-J, Thomas M, Langella P, Oswald E. 2021. A Toxic Friend: Genotoxic and
484 Mutagenic Activity of the Probiotic Strain Escherichia coli Nissle 1917. mSphere
485 6:e0062421.

486 20. Arthur JC, Perez-Chanona E, Mühlbauer M, Tomkovich S, Uronis JM, Fan T-J,
487 Campbell BJ, Abujamel T, Dogan B, Rogers AB, Rhodes JM, Stintzi A, Simpson KW,
488 Hansen JJ, Keku TO, Fodor AA, Jobin C. 2012. Intestinal inflammation targets cancer-
489 inducing activity of the microbiota. 6103. Science 338:120–123.

490 21. Arthur JC, Gharaibeh RZ, Mühlbauer M, Perez-Chanona E, Uronis JM, McCafferty J,
491 Fodor AA, Jobin C. 2014. Microbial genomic analysis reveals the essential role of
492 inflammation in bacteria-induced colorectal cancer. Nat Commun 5:4724.

493 22. Tronnet S, Garcie C, Rehm N, Dobrindt U, Oswald E, Martin P. 2016. Iron
494 Homeostasis Regulates the Genotoxicity of Escherichia coli That Produces Colibactin. Infect
495 Immun 84:3358–3368.

496 23. Chagneau CV, Garcie C, Bossuet-Greif N, Tronnet S, Brachmann AO, Piel J,
497 Nougayrède J-P, Martin P, Oswald E. 2019. The Polyamine Spermidine Modulates the
498 Production of the Bacterial Genotoxin Colibactin. mSphere 4:e00414-19.

499 24. Rehm N, Wallenstein A, Keizers M, Homburg S, Magistro G, Chagneau CV, Klimek
500 H, Revelles O, Helloin E, Putze J, Nougayrède J-P, Schubert S, Oswald E, Dobrindt U. 2022.

501 Two Polyketides Intertwined in Complex Regulation: Posttranscriptional CsrA-Mediated
502 Control of Colibactin and Yersiniabactin Synthesis in Escherichia coli. mBio e0381421.

503 25. Oliero M, Calvé A, Fragoso G, Cuisiniere T, Hajjar R, Dobrindt U, Santos MM. 2021.
504 Oligosaccharides increase the genotoxic effect of colibactin produced by pks+ Escherichia
505 coli strains. BMC Cancer 21:172.

506 26. Zheng L, Kelly CJ, Colgan SP. 2015. Physiologic hypoxia and oxygen homeostasis in
507 the healthy intestine. A Review in the Theme: Cellular Responses to Hypoxia. Am J Physiol
508 Cell Physiol 309:C350-360.

509 27. Brown AN, Anderson MT, Bachman MA, Mobley HLT. 2022. The ArcAB Two-
510 Component System: Function in Metabolism, Redox Control, and Infection. Microbiol Mol
511 Biol Rev 86:e00110-21.

512 28. Campbell EL, Bruyninckx WJ, Kelly CJ, Glover LE, McNamee EN, Bowers BE,
513 Bayless AJ, Scully M, Saeedi BJ, Golden-Mason L, Ehrentraut SF, Curtis VF, Burgess A,
514 Garvey JF, Sorensen A, Nemenoff R, Jedlicka P, Taylor CT, Kominsky DJ, Colgan SP. 2014.
515 Transmigrating neutrophils shape the mucosal microenvironment through localized oxygen
516 depletion to influence resolution of inflammation. Immunity 40:66–77.

517 29. McKeown SR. 2014. Defining normoxia, physoxia and hypoxia in tumours-
518 implications for treatment response. Br J Radiol 87:20130676.

519 30. Byndloss MX, Bäumler AJ. 2018. The germ-organ theory of non-communicable
520 diseases. Nat Rev Microbiol 16:103–110.

521 31. Cevallos SA, Lee J-Y, Tiffany CR, Byndloss AJ, Johnston L, Byndloss MX, Bäumler
522 AJ. 2019. Increased Epithelial Oxygenation Links Colitis to an Expansion of Tumorigenic
523 Bacteria. mBio 10:e02244-19.

524 32. Tronnet S, Floch P, Lucarelli L, Gaillard D, Martin P, Serino M, Oswald E. 2020. The
525 Genotoxin Colibactin Shapes Gut Microbiota in Mice. mSphere 5:e00589-20.

526 33. Tang-Fichaux M, Chagneau CV, Bossuet-Greif N, Nougayrède J-P, Oswald É,
527 Branchu P. 2020. The Polyphosphate Kinase of Escherichia coli Is Required for Full
528 Production of the Genotoxin Colibactin. mSphere 5:e01195-20.

529 34. Dubois D, Baron O, Cougnoux A, Delmas J, Pradel N, Boury M, Bouchon B, Bringer
530 M-A, Nougayrède J-P, Oswald E, Bonnet R. 2011. ClbP is a prototype of a peptidase
531 subgroup involved in biosynthesis of nonribosomal peptides. J Biol Chem 286:35562–35570.

532 35. Münch R, Hiller K, Grote A, Scheer M, Klein J, Schobert M, Jahn D. 2005. Virtual
533 Footprint and PRODORIC: an integrative framework for regulon prediction in prokaryotes.
534 Bioinformatics 21:4187–4189.

535 36. Mika F, Hengge R. 2005. A two-component phosphotransfer network involving ArcB,
536 ArcA, and RssB coordinates synthesis and proteolysis of sigmaS (RpoS) in E. coli. Genes
537 Dev 19:2770–2781.

538 37. Park SJ, Cotter PA, Gunsalus RP. 1995. Regulation of malate dehydrogenase (mdh)
539 gene expression in Escherichia coli in response to oxygen, carbon, and heme availability. J
540 Bacteriol 177:6652–6656.

541 38. Carreau A, El Hafny-Rahbi B, Matejuk A, Grillon C, Kieda C. 2011. Why is the
542 partial oxygen pressure of human tissues a crucial parameter? Small molecules and hypoxia. J
543 Cell Mol Med 15:1239–1253.

544 39. Albenberg L, Esipova TV, Judge CP, Bittinger K, Chen J, Laughlin A, Grunberg S,
545 Baldassano RN, Lewis JD, Li H, Thom SR, Bushman FD, Vinogradov SA, Wu GD. 2014.
546 Correlation between intraluminal oxygen gradient and radial partitioning of intestinal
547 microbiota. Gastroenterology 147:1055-1063.e8.

548 40. Brahimi-Horn MC, Pouysségur J. 2007. Oxygen, a source of life and stress. FEBS Lett
549 581:3582–3591.

550 41. Crofts AA, Giovanetti SM, Rubin EJ, Poly FM, Gutiérrez RL, Talaat KR, Porter CK,
551 Riddle MS, DeNearing B, Brubaker J, Maciel M, Alcala AN, Chakraborty S, Prouty MG,
552 Savarino SJ, Davies BW, Trent MS. 2018. Enterotoxigenic E. coli virulence gene regulation
553 in human infections. Proc Natl Acad Sci USA 115:E8968–E8976.

554 42. Marteyn B, West NP, Browning DF, Cole JA, Shaw JG, Palm F, Mounier J, Prévost
555 M-C, Sansonetti P, Tang CM. 2010. Modulation of Shigella virulence in response to available
556 oxygen in vivo. Nature 465:355–358.

557 43. Eberly AR, Floyd KA, Beebout CJ, Colling SJ, Fitzgerald MJ, Stratton CW, Schmitz
558 JE, Hadjifrangiskou M. 2017. Biofilm Formation by Uropathogenic Escherichia coli Is
559 Favored under Oxygen Conditions That Mimic the Bladder Environment. Int J Mol Sci
560 18:E2077.

561 44. Jiang F, An C, Bao Y, Zhao X, Jernigan RL, Lithio A, Nettleton D, Li L, Wurtele ES,
562 Nolan LK, Lu C, Li G. 2015. ArcA Controls Metabolism, Chemotaxis, and Motility
563 Contributing to the Pathogenicity of Avian Pathogenic Escherichia coli. Infect Immun
564 83:3545–3554.

565 45. Fischbach MA, Walsh CT, Clardy J. 2008. The evolution of gene collectives: How
566 natural selection drives chemical innovation. Proceedings of the National Academy of
567 Sciences 105:4601–4608.

568 46. Payros D, Secher T, Boury M, Brehin C, Ménard S, Salvador-Cartier C, Cuevas-
569 Ramos G, Watrin C, Marcq I, Nougayrède J-P, Dubois D, Bedu A, Garnier F, Clermont O,
570 Denamur E, Plaisancié P, Theodorou V, Fioramonti J, Olier M, Oswald E. 2014. Maternally
571 acquired genotoxic Escherichia coli alters offspring's intestinal homeostasis. 3. Gut Microbes
572 5:313–325.

573 47. Lucas C, Salesse L, Hoang MHT, Bonnet M, Sauvanet P, Larabi A, Godfraind C,
574 Gagnière J, Pezet D, Rosenstiel P, Barnich N, Bonnet R, Dalmasso G, Nguyen HTT. 2020.
575 Autophagy of Intestinal Epithelial Cells Inhibits Colorectal Carcinogenesis Induced by
576 Colibactin-Producing Escherichia coli in ApcMin/+ Mice. Gastroenterology 158:1373–1388.

577 48. Mohyeldin A, Garzón-Muvdi T, Quiñones-Hinojosa A. 2010. Oxygen in stem cell
578 biology: a critical component of the stem cell niche. Cell Stem Cell 7:150–161.

579 49. Lee-Six H, Olafsson S, Ellis P, Osborne RJ, Sanders MA, Moore L, Georgakopoulos
580 N, Torrente F, Noorani A, Goddard M, Robinson P, Coorens THH, O'Neill L, Alder C, Wang
581 J, Fitzgerald RC, Zilbauer M, Coleman N, Saeb-Parsy K, Martincorena I, Campbell PJ,

582 Stratton MR. 2019. The landscape of somatic mutation in normal colorectal epithelial cells.
583 Nature 574:532–537.

584 50. Dejea CM, Fathi P, Craig JM, Boleij A, Taddese R, Geis AL, Wu X, DeStefano
585 Shields CE, Hechenbleikner EM, Huso DL, Anders RA, Giardiello FM, Wick EC, Wang H,
586 Wu S, Pardoll DM, Housseau F, Sears CL. 2018. Patients with familial adenomatous
587 polyposis harbor colonic biofilms containing tumorigenic bacteria. 6375. Science 359:592–
588 597.

589 51. Melican K, Boekel J, Månsson LE, Sandoval RM, Tanner GA, Källskog Ö, Palm F,
590 Molitoris BA, Richter-Dahlfors A. 2008. Bacterial infection-mediated mucosal signalling
591 induces local renal ischaemia as a defence against sepsis. Cellular Microbiology 10:1987–
592 1998.

593 52. Nougayrède J-P, Homburg S, Taieb F, Boury M, Brzuszkiewicz E, Gottschalk G,
594 Buchrieser C, Hacker J, Dobrindt U, Oswald E. 2006. Escherichia coli induces DNA double-
595 strand breaks in eukaryotic cells. Science 313:848–851.

596 53. Rhee K-J, Cheng H, Harris A, Morin C, Kaper JB, Hecht G. 2011. Determination of
597 spatial and temporal colonization of enteropathogenic E. coli and enterohemorrhagic E. coli in
598 mice using bioluminescent in vivo imaging. Gut Microbes 2:34–41.

599 54. Pérez-Berezo T, Pujo J, Martin P, Le Faouder P, Galano J-M, Guy A, Knauf C, Tabet
600 JC, Tronnet S, Barreau F, Heuillet M, Dietrich G, Bertrand-Michel J, Durand T, Oswald E,
601 Cenac N. 2017. Identification of an analgesic lipopeptide produced by the probiotic
602 Escherichia coli strain Nissle 1917. Nat Commun 8:1314.

603 55. Zhou K, Zhou L, Lim Q 'En, Zou R, Stephanopoulos G, Too H-P. 2011. Novel
604 reference genes for quantifying transcriptional responses of Escherichia coli to protein
605 overexpression by quantitative PCR. BMC Mol Biol 12:18.

606
607

608 **Figures**
609

610

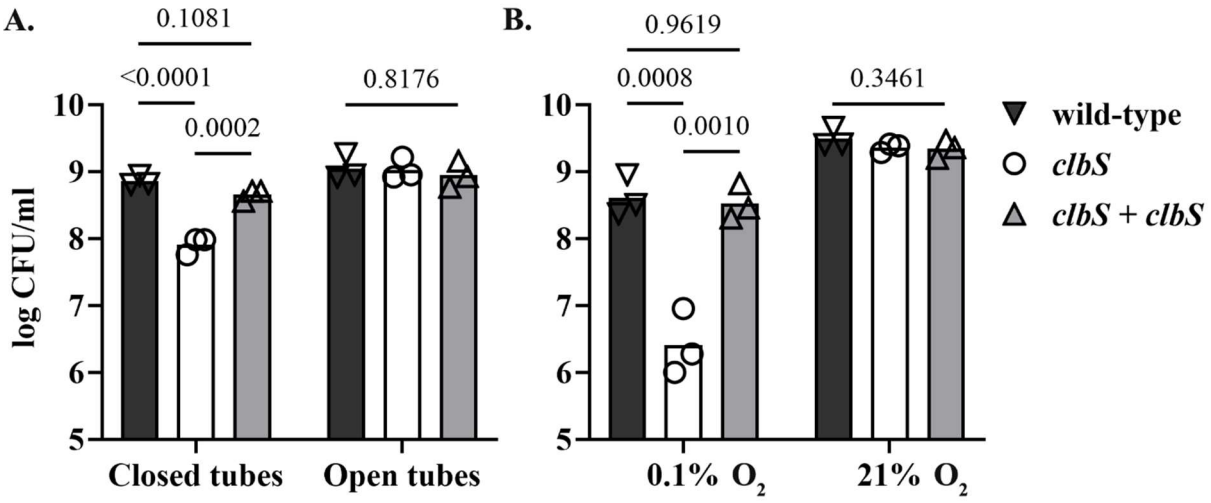

611

612

613 **Figure 1: Culture oxygenation modulates the autotoxicity phenotype of a *clbS* mutant in**
614 **a *pks*+ *E. coli*.**
615 **A**. *E. coli* strain DH10B pBAC*pks*, the isogenic *clbS* mutant deficient for colibactin self-
616 resistance protein, and the trans-complemented *clbS* mutant (*clbS* + *clbS*), were grown (5 ml
617 LB) with shaking in a standard atmospheric incubator, in 10 ml tubes that were tightly closed,
618 or in 50 ml tubes with the cap opened. **B.** The bacteria were cultured with shaking in tubes with
619 cap in vented position, within a hypoxic chamber at 0.1% O_2, or in a standard atmosphere
620 incubator (21% O_2).
621 After 16 h culture, bacterial growth was determined by plating and counting colony forming
622 units (CFU). The mean and individual results of three independent experiments are shown, with
623 the p values of an ANOVA and Tukey's multiple comparison test.
624

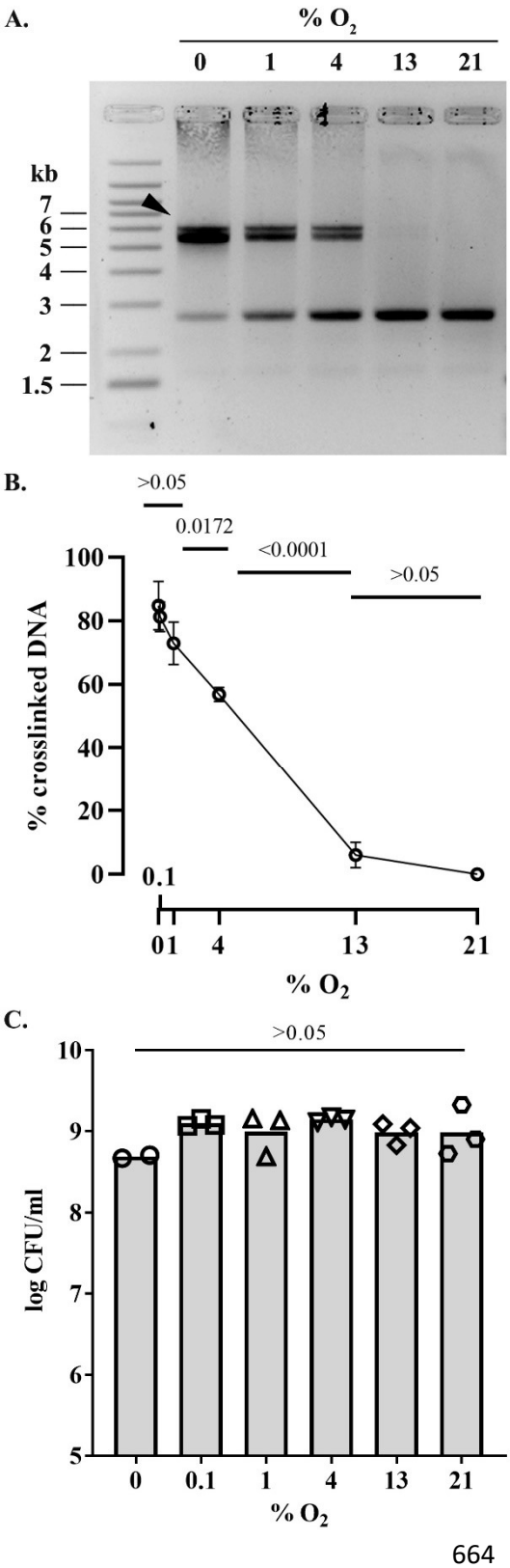

Figure 2: Effect of oxygen concentration on the DNA crosslinking activity of a *pks+ E. coli.*

A. Linearized plasmid DNA was exposed 40 min to the *pks+ E. coli* strain SP15 grown 3.5 hours with shaking in vented cap tubes within an incubator regulated at the given percentage of oxygen, and then analyzed by denaturing gel electrophoresis. The sizes of the DNA fragments in the ladder are noted in kilobase. The DNA cross-linked by colibactin with apparent doubling in size compared to the intact denatured DNA is shown with an arrow.

B. The percentage of DNA signal in the upper, crosslinked DNA relative to the total DNA signal in the lane was determined by image analysis. The mean and standard error of three independent experiments are shown, with the p values of an ANOVA and Tukey's multiple comparison test.

C. In the same experiments, the bacterial growth following 3.5 hours culture at given percentages of oxygen was examined by plating and counting colony forming units (CFU).

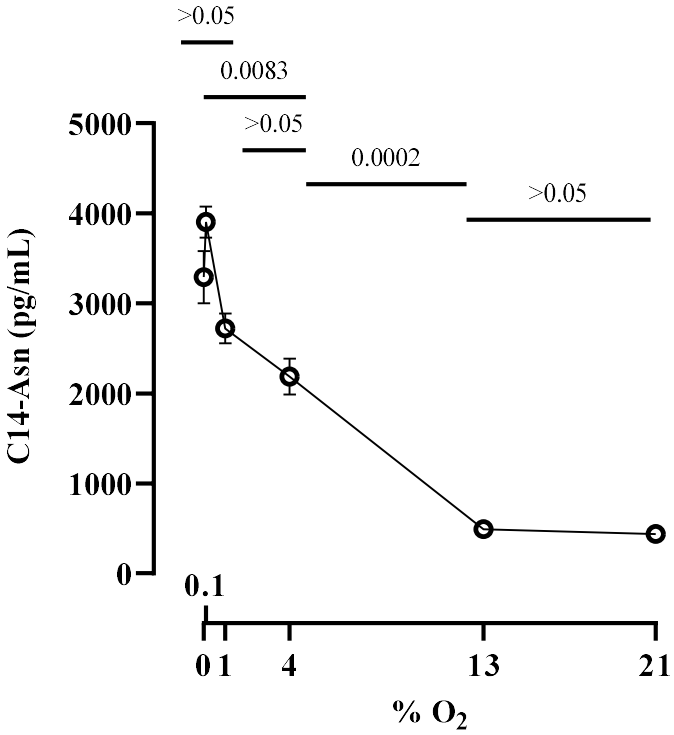

Figure 3 : Effect of oxygen concentration on the production of colibactin cleavage product C14-Asn.

The *E. coli* strain SP15 was grown 3.5 hours with shaking in vented tubes in an incubator regulated at various percentage of oxygen, then the culture supernatants were collected, the lipids were extracted and colibactin cleavage product C14-Asn was quantified by liquid chromatography coupled to mass spectrometry. The mean and standard error of three independent cultures are shown, with the p values of an ANOVA and Tukey's multiple comparison test. The error bars of the biological triplicate samples at $\%O_2$>=13% are too small to appear on the graph.

677

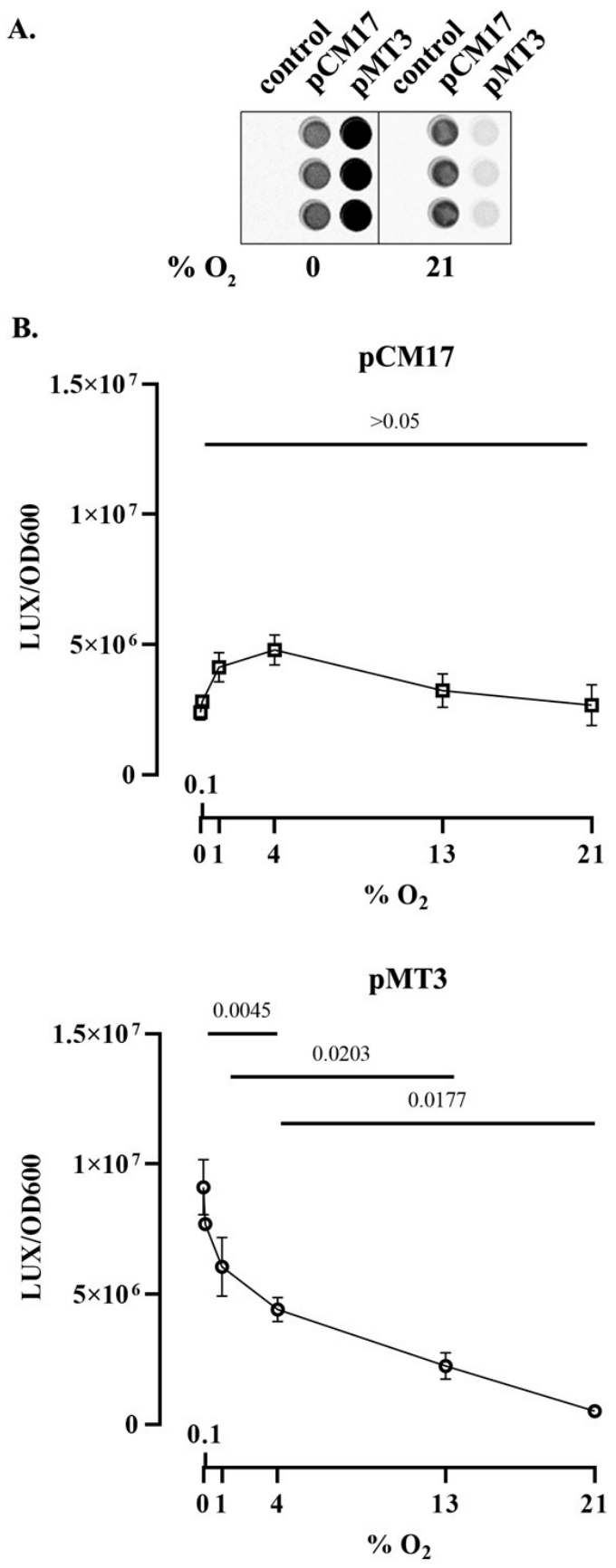

Figure 4 : Effect of oxygen concentration on *clbB* promoter activity.

A. Luminescence of *E. coli* strain SP15 carrying the luciferase reporter plasmid pCM17 or pMT3 (constitutive promoter or *clbB* promoter upstream of *luxCDABE* respectively), or the plasmid without promoter as a control. Three independent bacterial cultures grown 3.5 h at 0% or 21% oxygen were placed in a 96-well microplate and photographed with a CCD camera in a dark imaging station. Atmospheric oxygen present during the image acquisition provide the oxygen required to the reaction catalyzed by the luciferase.

B. The luminescence (normalized to the optical density at 600 nm) was measured in a plate reader following 3.5 hours culture at specified percentages of oxygen. The mean and standard error of three independent cultures are shown, with the p values of an ANOVA and Tukey's multiple comparison test.

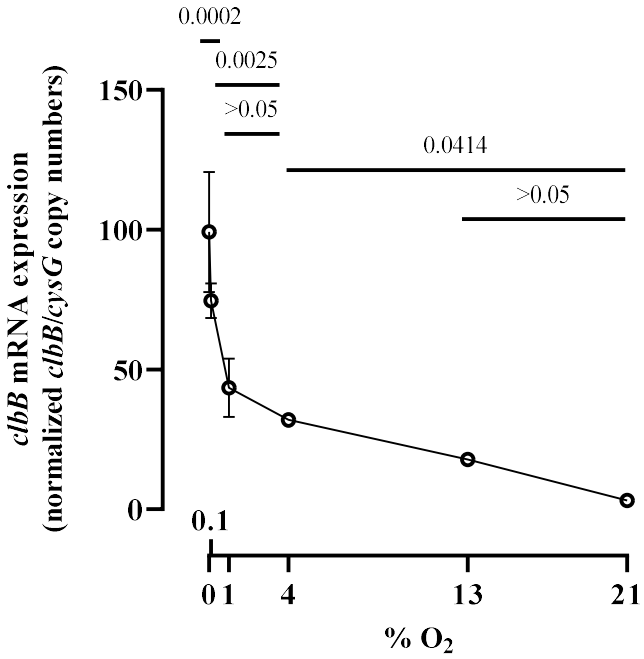

708
709
710
711 **Figure 5 : Effect of oxygen concentration on *clbB* gene expression.**
712 The mRNA levels of *clbB* gene were determined in *E. coli* SP15 grown 3.5 hours at specified
713 percentages of oxygen. The DNA copy number of the *clbB* mRNA relative to that of the *cysG*
714 housekeeping gene was normalized to the mean maximum level. The mean and standard error
715 of three independent cultures are shown, with the p values of an ANOVA and Tukey's multiple
716 comparison test. The error bars of the biological triplicate samples at O_2>=4% are too small to
717 appear on the graph.
718
719
720
721

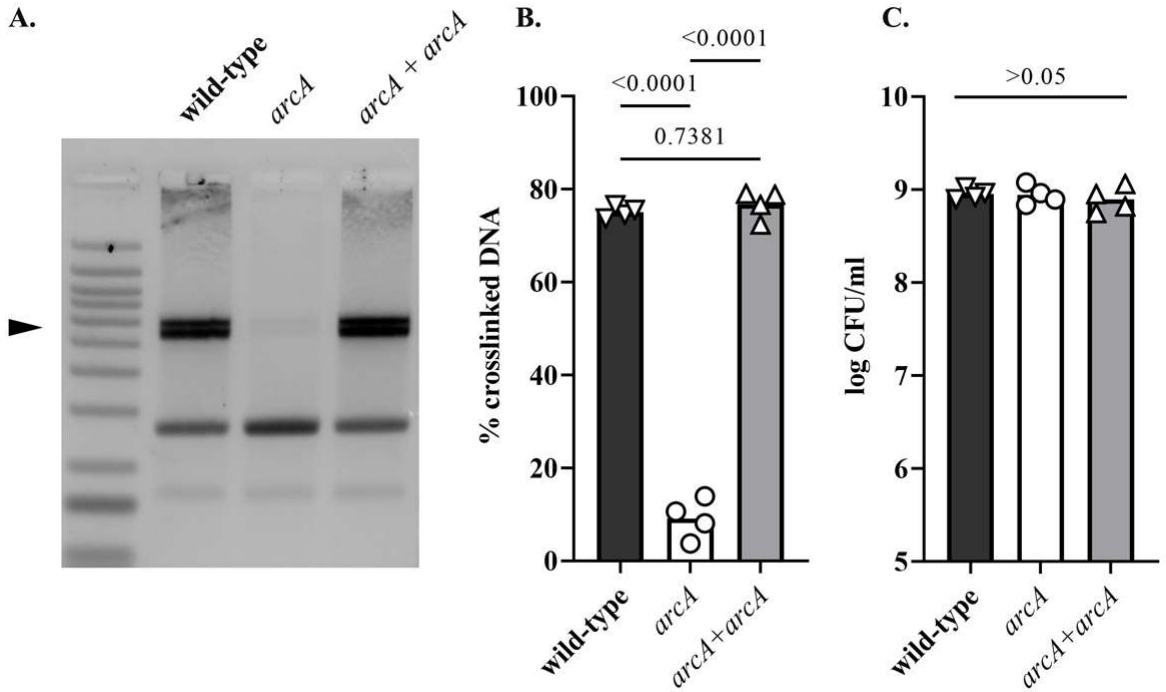

Figure 6: Deletion of *arcA* results in decreased DNA crosslinking activity of a *pks*+ *E. coli.*
A. *E. coli* wild-type strain SP15, *arcA* mutant and *arcA* mutant complemented with a plasmid-encoded *arcA* were grown 3.5 hours at 0.1% oxygen, then incubated 40 min with linearized plasmid DNA. The DNA cross-linked by colibactin with apparent doubling in size (arrow) was visualized by denaturing gel electrophoresis. The sizes of the DNA fragments in the ladder are depicted in figure 2A.
B. The percentage of DNA signal in the crosslinked DNA band relative to the total DNA signal in the lane was determined by image analysis. The results of four independent cultures are shown, with the p values of an ANOVA and Tukey's multiple comparison test.
C. In the same experiments, the bacterial growth following 3.5 hours culture was examined by plating and counting colony forming units (CFU).

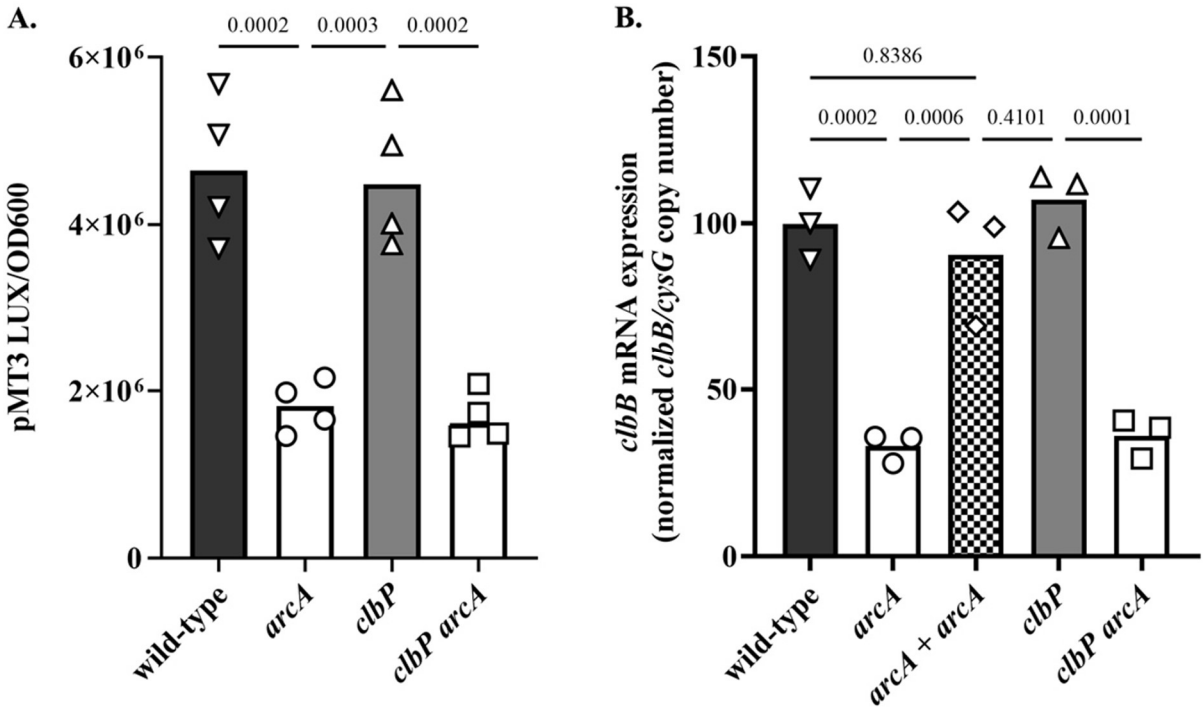

Figure 7: Effect of *arcA* mutation on *clbB* promoter activity and *clbB* expression.

A. Luminescence of the *E. coli* wild-type strain SP15, the *arcA* mutant, *clbP* mutant or *clbP arcA* double mutant carrying the luciferase reporter plasmid pMT3 (encoding the promoter region of *clbB* upstream of *luxCDABE*) grown 3.5 h at 0.1% O_2. The luminescence (normalized to the optical density at 600 nm) of four independent bacterial cultures grown 3.5 h at 0.1% O_2 was measured in a plate reader. The mean and individual values are shown, with the p values of an ANOVA and Tukey's multiple comparison test.

B. The mRNA levels of the *clbB* gene were determined in *E. coli* wild-type strain SP15, the *arcA* mutant, the complemented *arcA* mutant (*arcA* + *arcA*), the *clbP* mutant or *clbP arcA* double mutant grown 3.5 h at 0.1% O_2. The DNA copy number of the *clbB* mRNA relative to that of the *cysG* housekeeping gene was normalized to the mean wild-type level. The mean and individual values of independent cultures are shown, with the p values of an ANOVA and Tukey's multiple comparison test.

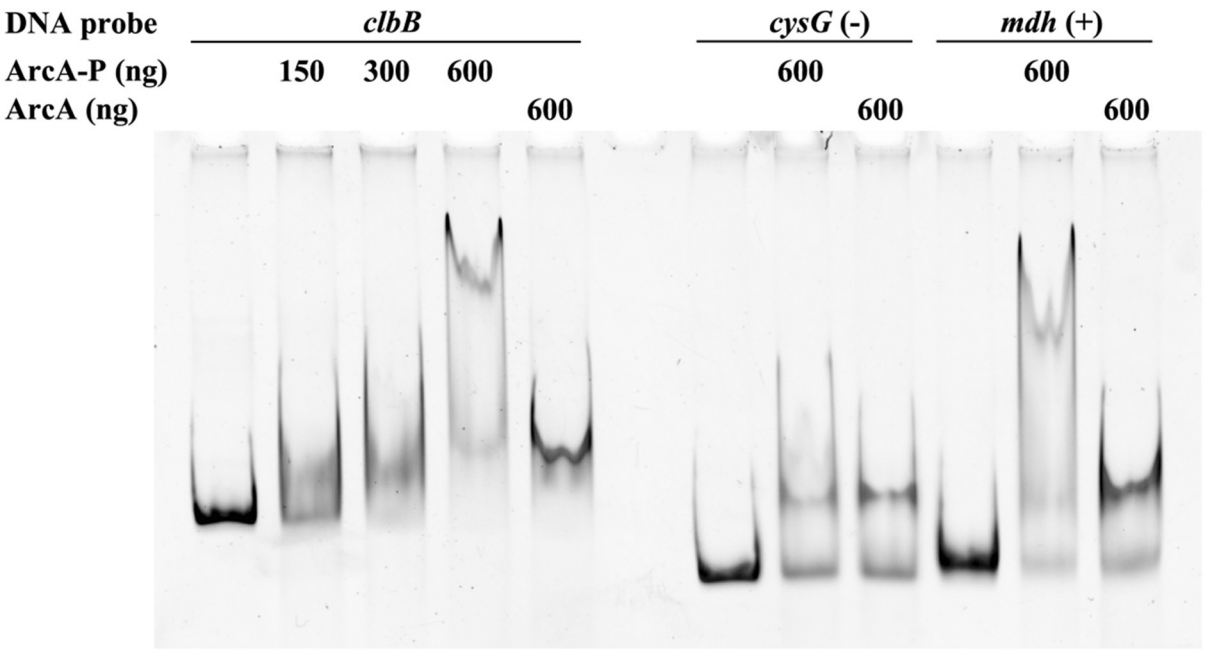

750
751
752 **Figure 8: phosphorylated ArcA binds to *clbB* promoter region.**
753 EMSA using a DNA probe carrying the *clbB* promoter region and purified ArcA-P
754 (phosphorylated *in vitro*) or ArcA, in indicated amounts. DNA probes carrying a *cysG*
755 intragenic region or *mdh* promoter region were used as negative and positive controls,
756 respectively.
757

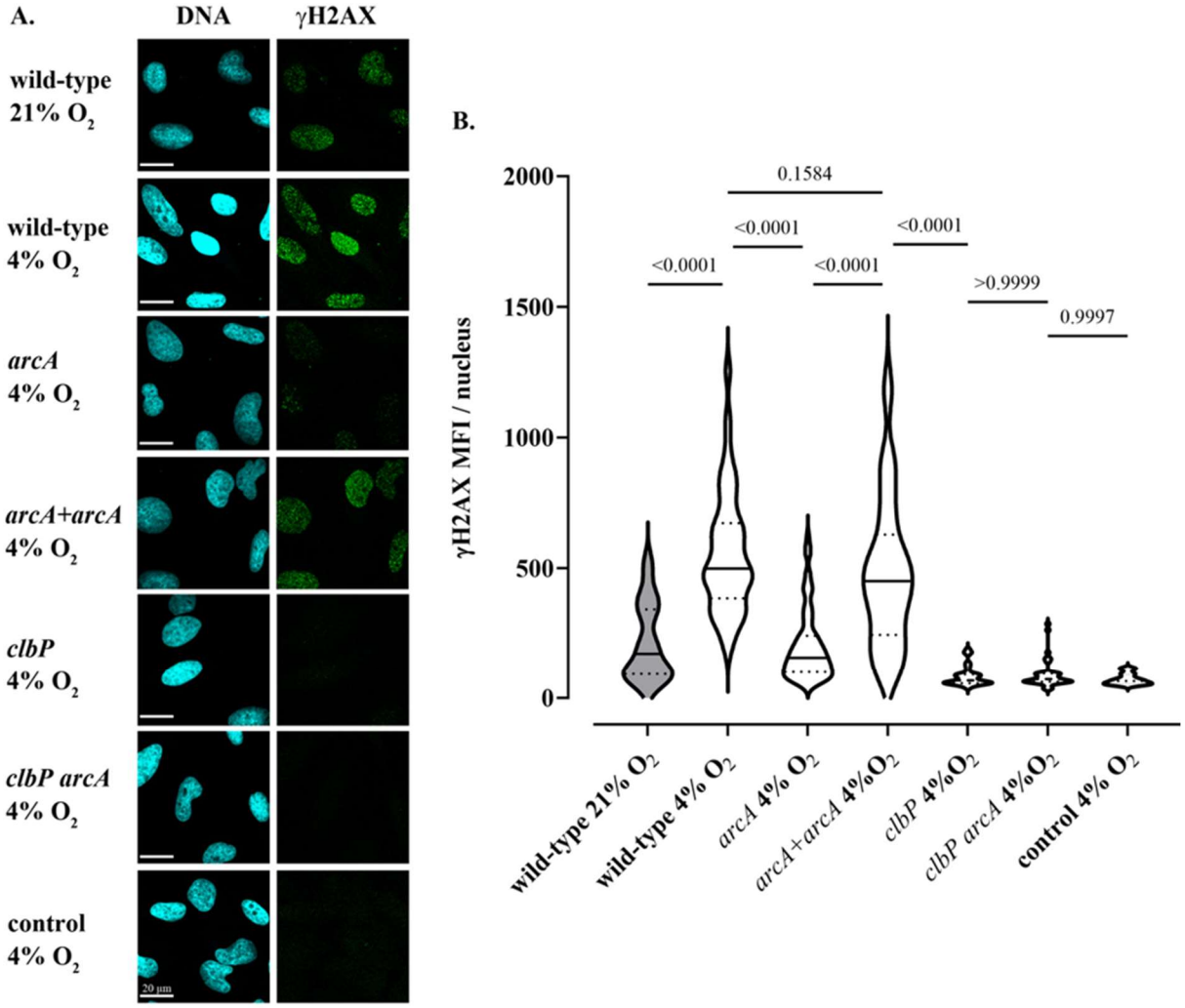

Figure 9: Oxygen and the *arcA* mutation inhibit the genotoxicity of colibactin-producing *E. coli*.

A. HeLa epithelial cells were infected with *E. coli* wild-type strain SP15, the *clbP* mutant, the *arcA* mutant, the *arcA* mutant complemented with plasmid-encoded *arcA,* or the *clbP arcA* double mutant for 4 hours under 21% or 4% oxygen atmosphere, and then cellular DNA-damage was detected by γH2AX immunofluorescent staining. DNA was counterstained with DAPI. Scale bar = 20 µm

B. γH2AX mean fluorescence intensity (MFI) within approximatively 40 to 90 cell nuclei in 2 to 4 independent experiments was measured by image analysis. The violin plots show the frequency distribution of the data, with the median and quartiles as solid and dotted lines. P values were calculated with an ANOVA and Tukey's multiple comparison test.

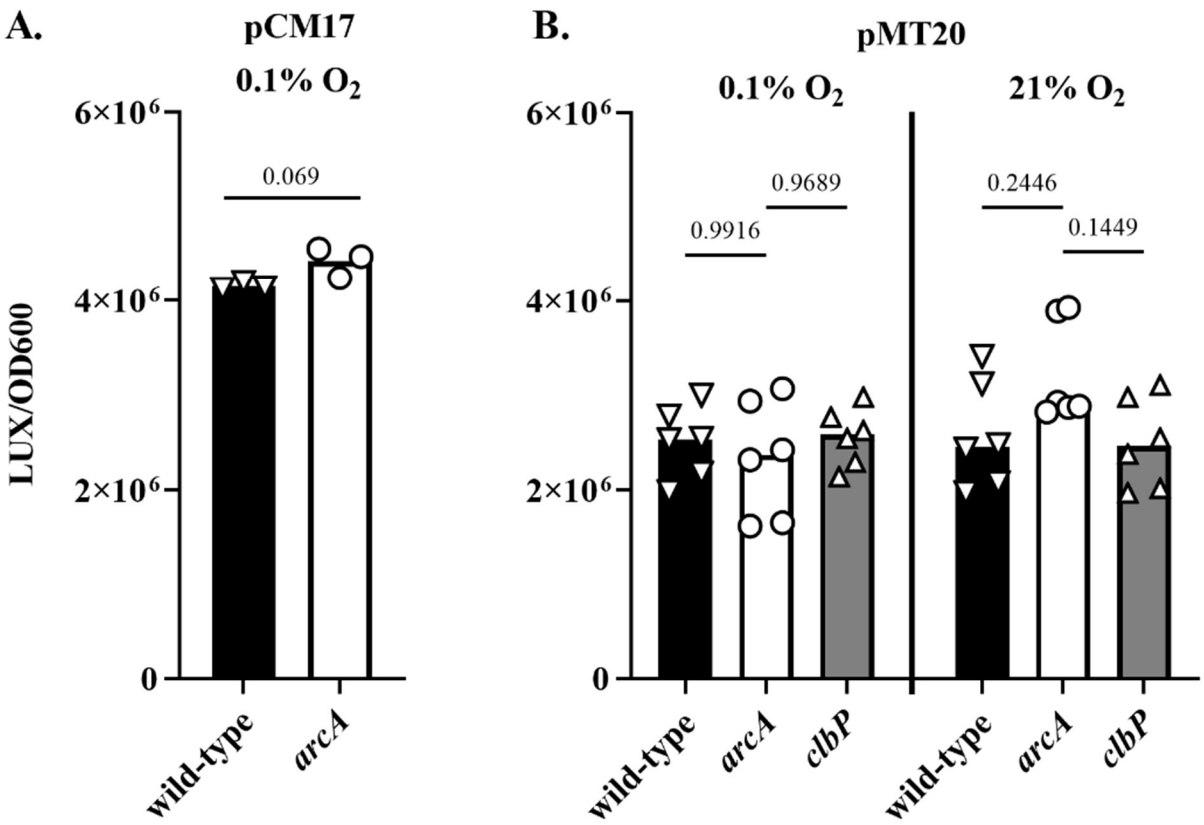

Supplementary figure 1:

A. Luminescence of *E. coli* strain SP15 carrying the luciferase reporter plasmid pCM17 (constitutive promoter upstream of *luxCDABE*) grown 3.5 h at 0.1% oxygen. The mean and individual values of three independent cultures are shown, with the p value of a t-test.

B. Luminescence of *E. coli* strain SP15 carrying the luciferase reporter plasmid pMT20 (promoter region of *clbS* upstream of *luxCDABE*) grown 3.5 h at 0.1% or 21% oxygen. The mean of 6 independent cultures are shown, with the p values of an ANOVA and Tukey's multiple comparison test.

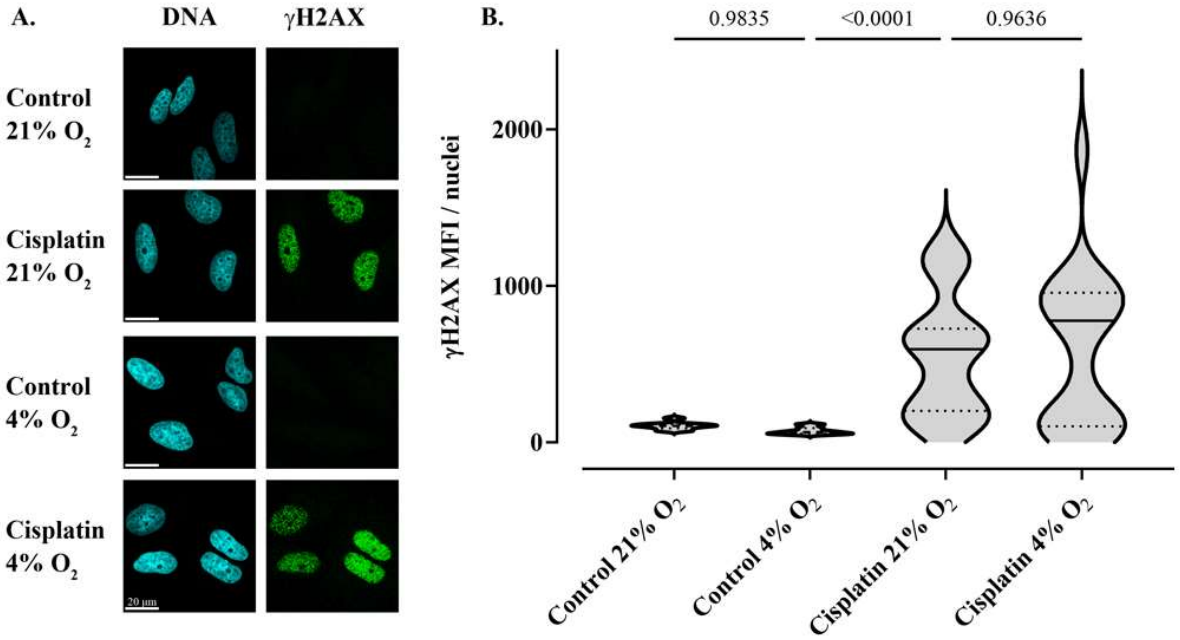

Supplementary figure 2: Oxygen does not alter the γH2AX response of genotoxin-treated HeLa cells.

A. HeLa epithelial cells were treated with cisplatin for 4 hours under 21% ("hyperoxic") or 4% ("normoxic") oxygen atmosphere, and then cellular DNA-damage was demonstrated by γH2AX immunofluorescent staining. DNA was counterstained with DAPI. Scale bar = 20 µm

B. γH2AX mean fluorescent intensity (MFI) within ~50 cell nuclei was measured by image analysis. The violin plots show the frequency distribution of the data, with the median and quartiles as solid and dotted lines. P values were calculated with an ANOVA and Tukey's multiple comparison test.

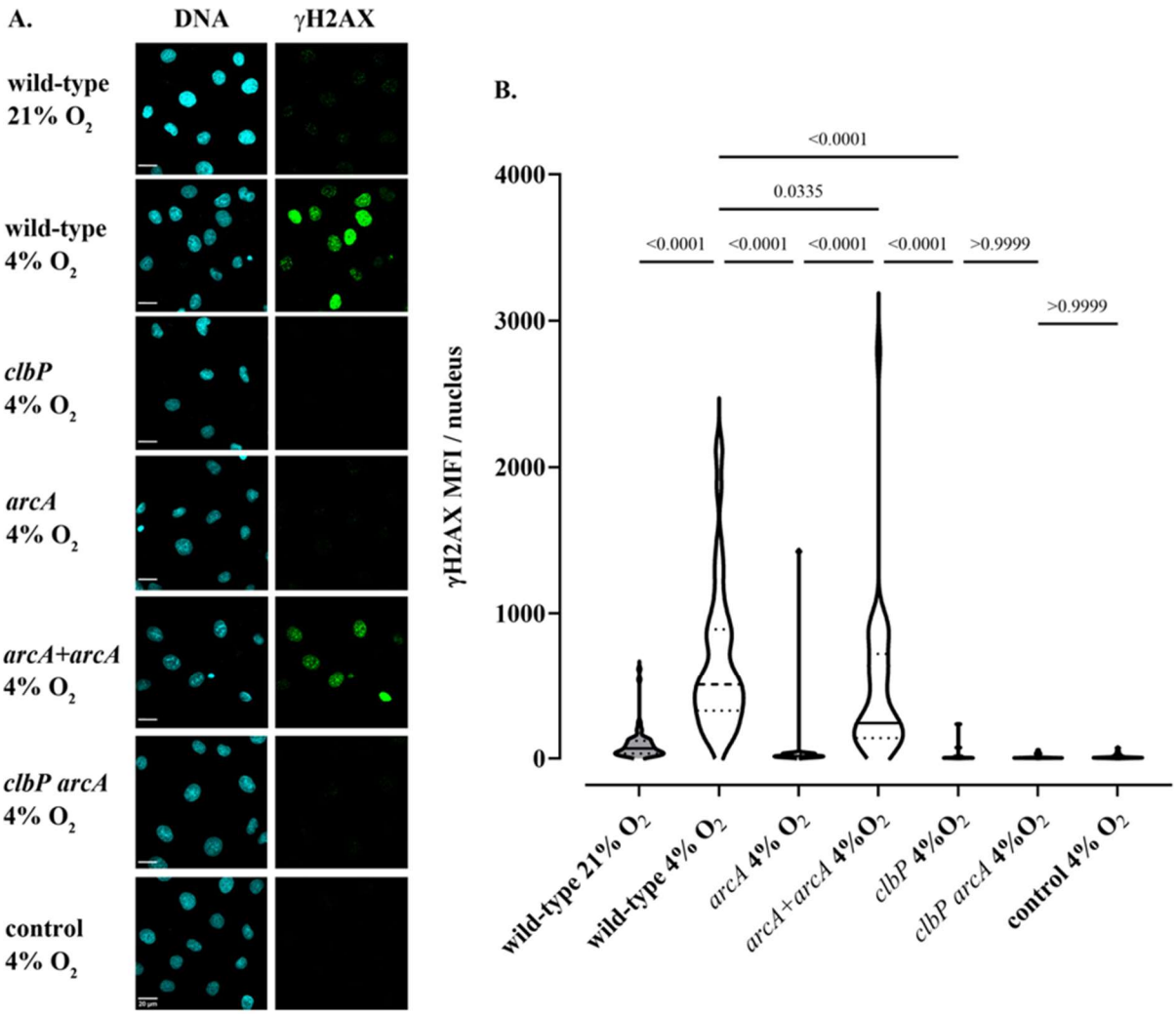

Supplementary figure 3: High oxygen concentration and *arcA* deletion inhibit the genotoxicity of colibactin-producing *E. coli* in intestinal IEC-6 cells.

A. Non-transformed rat intestinal epithelial IEC-6 cells were infected with *E. coli* wild-type strain SP15, the *clbP* mutant, the *arcA* mutant, the *arcA* mutant complemented with plasmid-encoded *arcA,* or the *clbP arcA* double mutant for 4 hours under 21% or 4% O_2 atmosphere and then cellular DNA-damage was detected by γH2AX immunofluorescence staining. DNA was counterstained with DAPI. Scale bar = 20 µm

B. γH2AX mean fluorescence intensity (MFI) within approximatively 60 nuclei was measured by image analysis. The violin plots show the frequency distribution of the data, with the median and quartiles as solid and dotted lines. P values were calculated with an ANOVA and Tukey's multiple comparison test.

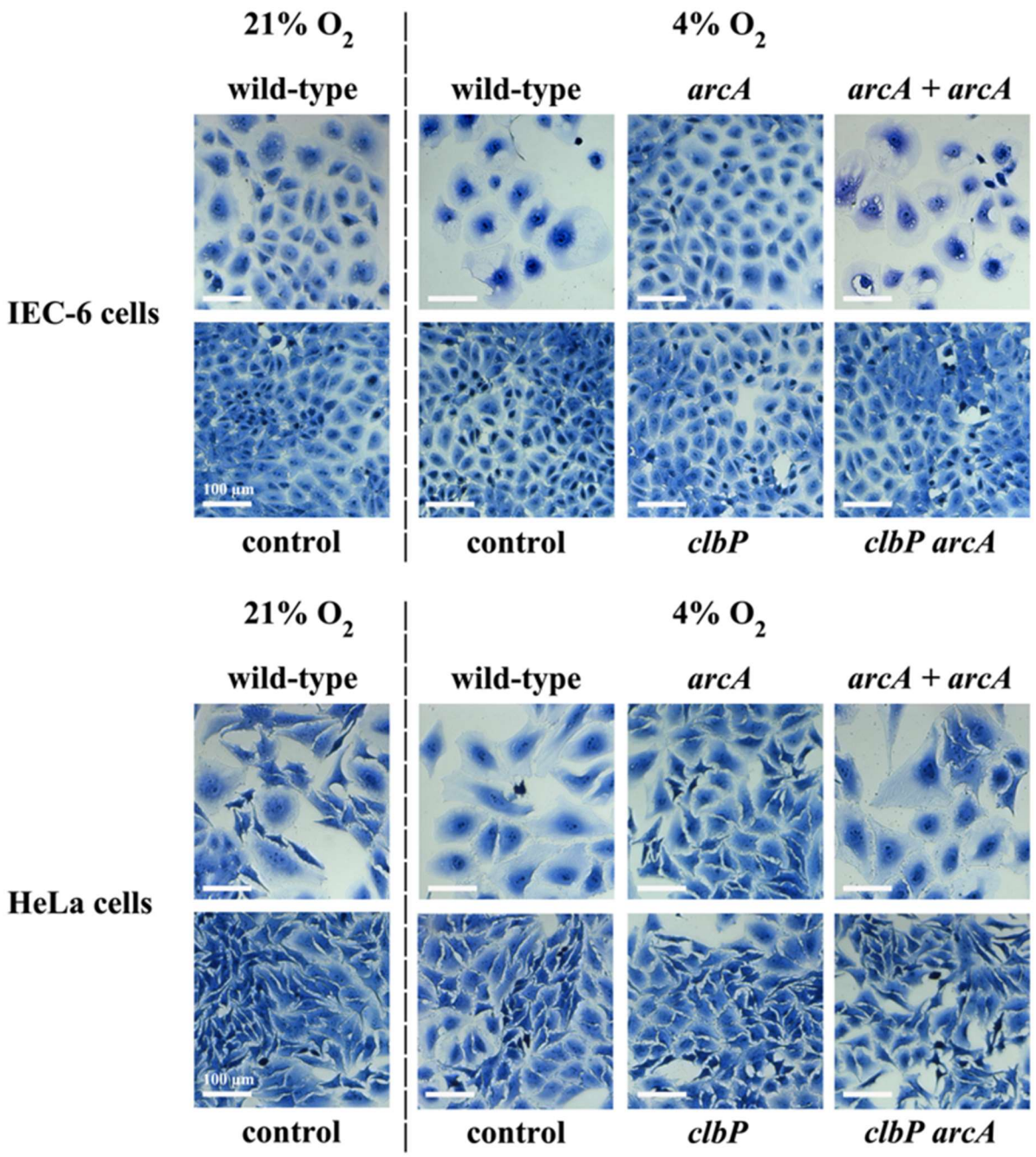

Supplementary figure 4: Cytotoxicity phenotype observed in IEC-6 and HeLa cells 48 h after infection with *E. coli* wild-type strain SP15, the *arcA* mutant, the *arcA* mutant complemented with plasmid-encoded *arcA,* the *clbP* mutant or the *clbP arcA* double mutant, under 21% or 4% O_2 atmosphere. Control cells were left non-infected. Scale bars = 100 µm.